Identifying the electrical signature of snow in photovoltaic inverter data

Emma C. Cooper, Jennifer L. Braid, and Laurie M. Burnham
Sandia National Laboratories, Albuquerque, NM, 87106, USA

***Abstract*—Snow is a significant challenge for PV plants at northern latitudes, and snow-related power losses can exceed 30% of annual production. Accurate loss estimates are needed for resource planning and to validate mitigation strategies, but this requires accurate snow detection at the inverter level. In this study, we propose and validate a framework for detecting snow in time-series inverter data. We identify four distinct snow-related power loss modes based on the inverter's operating points and electrical properties of the inverter and PV arrays. We validate these modes and identify their associated physical snow conditions using site images. Finally we examine relative frequencies of the snow power loss modes and their contributions to total power loss.**

I. Introduction

As penetration of renewable energy generation increases, seasonal mismatches between renewable production and demand are becoming increasingly problematic [1]. Many studies have demonstrated that snow significantly compromises PV output during winter [2]–[4], often a period of high demand in snowy regions [5], with losses as high as 90% - 100% during winter months for some systems [2], [6], [7]. Quantitative comparisons of designs that promote system resiliency against snow and fast snow shedding are needed, which require accurate estimates of snow losses [8].

Established methods for estimating snow loss can be grouped into data-driven models and physics-based models. The accuracy of stochastic or curve-fitting models has not been rigorously tested, but snow-cover models have been more thoroughly reviewed. Snow cover models can reduce error in generation predictions to as little as 7% during winter months, but reviews have demonstrated that these models tend to significantly underpredict snow losses if they do not reference current snow cover conditions [2]. Timeseries images can be used to provide snow cover conditions for these models, but implementation require advance planning and additional monitoring capabilities.

Over 30% of operable utility-scale fixed-tilt capacity is located in the U.S. at or above 40 degrees of latitude (as of 2021) [9], and represent vast stores of high quality performance and irradiance data collected in cold climates. An accurate method for identifying snow in these utility scale datasets would make snow loss quantification vastly more accessible to asset owners. Characterizing the electrical signature of snow has been the subject of simulation-based studies, but there has been little research with regard to analysis and identification in field data.

Snow losses were simulated for a single module with varying spatial coverage and snow transmissivity by [10], but models were not validated through field data. IV curves of shaded and unshaded modules connected in series were modeled as a function of shading coverage and validated through field data by [11], but the effect of transmission was not investigated. A recent study [12] developed an algorithm for identifying snow using inverter and onsite ambient temperature data, but comparison with field data demonstrated that the algorithm failed to detect a third of snow events.

In this study, we propose and validate a model for identifying snow in utility-scale PV inverter data with the goal of establishing the foundation for a utility-scale snow loss estimate tool. We use performance models to determine effective transmission and coverage from field data, and corroborate these values with site images. We use these parameters to introduce a framework for behaviors that are distinguishable within utility-scale field data and identify four distinct power-loss modes. We validate the presence of these modes across different system scales and data resolutions. We identify the physical snow cover situations that each mode corresponds to, and note differences across systems. We determine the relative frequencies of each mode and associated fraction of total power loss for each system, and correlate the aggregated results with panel orientation.

II. Methods

A. Data

A fifteen-minute resolution dataset for a monofacial fixed low-tilt utility-scale site was provided by an electric utility in Northeastern US, including 196 days from December 2020 to February 2022. The site was chosen because of the heavy snow losses observed by its asset owners; over the period of observation, the site experienced over 100 inches of snowfall and persistent snow cover on panels was observed to last for weeks on end.

Available data included inverter-level DC and AC voltage and combiner-level DC current as measured by a Solectria Yakasawa inverter, back-of-module (BOM) temperature, and plane-of-array (POA) irradiance measured by a heated pyranometer. Data was filtered using procedures outlined in

Sandia National Laboratories is a multimission laboratory managed and operated by National Technology & Engineering Solutions of Sandia, LLC, a wholly owned subsidiary of Honeywell International Inc., for the U.S. Department of Energy's National Nuclear Security Administration under contract DE-NA0003525. This work was supported by the U.S. Department of Energy's Office of Energy Efficiency and Renewable Energy (EERE) under the Solar Energy Technologies Office under Award 38527.

[13]. Additionally, periods of time where AC power output approached the inverter's nameplate limits were excluded to avoid clipped data. Site images showing a string of modules connected to an inverter were collected at 1-hour and 15-minute resolution (Fig. 1). Spatial coverage of snow on the string of modules was determined through an unsupervised pixel clustering algorithm [14] and used as a point of comparison to effective coverage as calculated using electrical data.

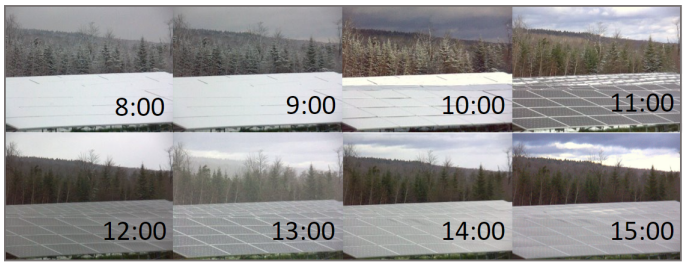

Fig. 1. One of the series of site images used to calculate snow cover, where a shedding event occurs between 10 am and 11 am.

B. Snow detection framework

For this work, we assume that a reduction in current or voltage performance index (PI) is due to light-blocking matter (here snow) on the surface of the modules. The electrical configuration of the site was typical in that modules were connected in series strings, which were connected in parallel at combiners. The current is measured at the combiner level, and is equivalent in magnitude to the module current multiplied by the number of module strings in parallel. Combiners are connected in parallel at the inverter, where voltage is measured and is equivalent in magnitude to the voltage of a string of modules. As a result, measured combiner current I_{mp} is representative of the average lowest nonzero current generated by a cell among parallel-connected module strings. Therefore, we estimate the effective transmission of light-blocking matter on the array, T_{eff}, as the fraction of light received by the panels, using the Sandia Array Performance Model (SAPM) [15] with combiner current, and onsite irradiance and BOM temperature data:

$$I_{mp} = N_{strings} \times I_{mp0}(C_0 E_e T_{eff} + C_1 (E_e T_{eff})^2) \times (1 + \alpha_{Imp}\,(T_{cell} - T_0)) \quad (1)$$

where C is a vector of coeffients specific to the module type, E_e is effective irradiance, T_{cell} is cell temperature, T_0 is 25 °C, I_{mp0} is the nameplate I_{mp} of the module, and $N_{strings}$ is the number of strings connected in parallel.

Inverter voltage was also modeled using the SAPM,

$$V_{mp} = N_{modules} \times [V_{mp0} + C_2\, N_s\, \delta \ln(E_e T_{eff}) + C_3\, N_s\, (\delta \ln(E_e T_{eff}))^2 + \beta_{Vmp}\,(T_{cell} - 25)] \quad (2)$$

using T_{eff} and sensor data, where N_s is the number of cells connected in series per module, V_{mp0} is the nameplate V_{mp} of the module, and $N_{modules}$ is the number of modules in a string.

Given that string operating voltage increases approximately linearly with the number of active (unbypassed) module substrings connected in series, the voltage PI, V_{ratio}, is representative of the average effective snow-free fraction of all PV strings connected to the inverter. The complement of V_{ratio} can be used a measure of effective coverage C_{eff}. In this framework, $V_{ratio} < 1$ corresponds to conditions where there are inactive substrings (activated bypass diodes) in the string, whereas $V_{ratio} \approx 1$ suggests that all substrings are active. A phase diagram of V_{ratio} is plotted against spatial coverage in Figure 2. The 540 V turn-on voltage (V_{turnon}) of site's inverter ensures that the system remains off unless $\approx 73\%$ of modules are operating at maximum power point (MPP), so it should be noted that $V_{ratio} < V_{turnon}/V_{mp0}$ will result in $C_{eff} = 1$. A decrease in transmission appears as a gradient from red to blue and is correlated with spatial coverage; as spatial coverage increases past $(1 - V_{turnon}/V_{mp0}) \times 100\%$, a non-zero V_{ratio} can only be measured for a system where light transmits through the snow and $T_{eff} < 1$.

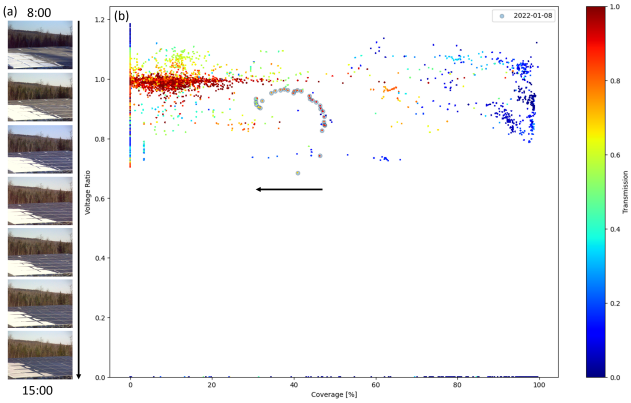

Fig. 2. (a) Images of the utility-scale site from 2022-01-08 where snow recedes from the panels over the course of the day. (b) V_{ratio} plotted against spatial coverage as determined through images. Points are colored by a calculated effective transmission where red indicates $T_{eff} \approx 1$ and blue indicates a lower T_{eff}; data from 2022-01-08 is highlighted to show a decrease in coverage and a corresponding increase in voltage PI.

Four power-loss modes corresponding to the electrically distinguishable behaviors discussed above are identified in Fig. 3. Mode 0 corresponds to a complete outage where the system does not meet the minimum turnon voltage for the inverter. Modes 1 and 2 describe data collected when one or more substrings are bypassed; Mode 1 is the case where the active substrings are limited in current due to less than 100% light transmission of snow, while Mode 2 is for active substrings operating as if uncovered by snow. Mode 3 corresponds to instances where all substrings are active but there is low effective transmission (current is limited due to snow cover). The cutoff values to distinguish between these modes were determined statistically from snow-free data to ensure normal operation was not classified as snow cover.

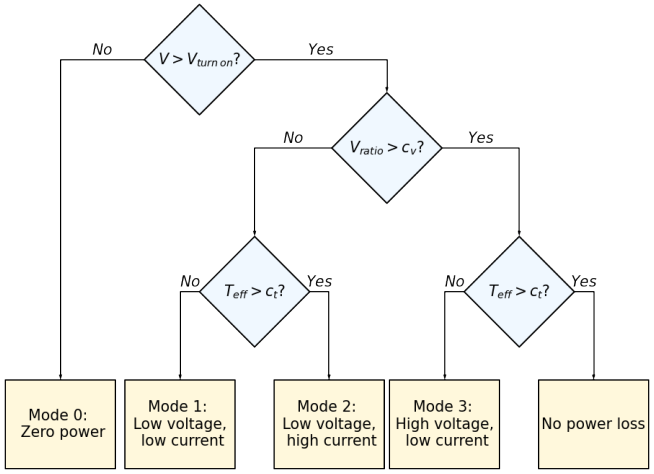

Fig. 3. Flowchart for determining power loss modes. Values for c_v and c_t were determined by identifying the 95th percentile of effective coverage and transmission in snow-free data.

TABLE I
RESEARCH-SCALE VALIDATION SITES

System	**String-inverter**	**Portrait-orientation module**	**Landscape-orientation module**
Voltage resolution	Inverter	Module	Module
Current resolution	Inverter	Module	Module
Orientation	Portrait	Portrait	Landscape
Date range	Nov. 2021 - Apr. 2023	Feb. - May 2023	Feb. - May 2023
Data frequency	1 minute	1 minute	1 minute
	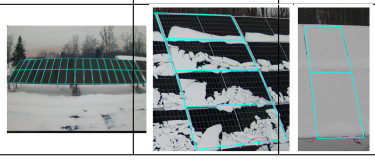		

C. Validation

Three monofacial research-scale systems at the Michigan Regional Test Center (MI-RTC) were selected for analysis based on their similarity to or differences from the utility-scale system (Table I). Single module systems were selected to verify the presence of power loss modes at a module-level, while a string-inverter system was selected for its structural similarity to the utility-scale system. Both portrait and landscape-orientation systems were included to isolate the effect of orientation on modal frequency. All systems were outfitted with at least one BOM thermocouple and POA irradiance was collected by a heated Kipp & Zonen pyranometer.

Phase diagrams for all three validation sites displayed a correlation between T_{eff} and spatial coverage similar to that seen for the utility-scale site. The two module-scale systems displayed markedly different patterns in voltage ratios; while the plot for the landscape-orientation module shows the number of individual substrings that are online (Figure 4a), the same is not apparent in the plot for the portrait-orientation module (Figure 4b). This is consistent with snow typically shedding down the length of a module, so that individual substrings on the upper half of a landscape orientation module can remain completely uncovered and online even while there is partial snow cover on the bottom portion of the module. The same is not true for a landscape-orientation module, as all substrings remain partially covered even if the upper portion of the panel is uncovered.

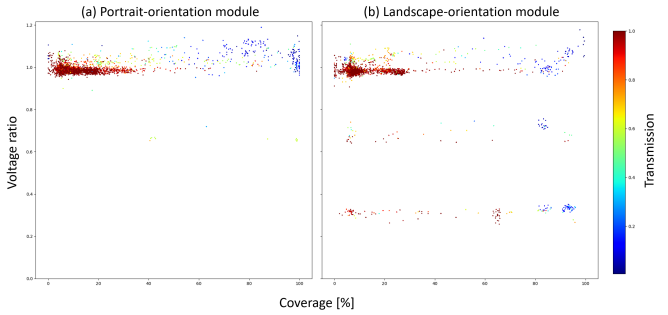

Fig. 4. Relative frequencies of modes for data collected between October and May that includes significant power losses. Data from mode 0 is not collected for the two module-scale systems, but an analysis of missing timestamps found that the portrait-orientation system was offline for ≈ 13 hours longer than the landscape-orientation system.

III. RESULTS

The electrical/optical characteristics and physical interpretations of power loss modes are summarized in Table II.

The relative frequencies and % power loss of modes across the utility-scale and validation sites are shown for periods of time when a power loss mode is present in Figure 6. For all data collected between the months of October and May during daylight hours, the utility-scale site experienced a snow-related power loss mode for 59% of recorded timestamps and the string-inverter system experienced the same for 52% of timestamps. These statistics are not intended for cross-site comparison, but more so to demonstrate the sheer magnitude of time that these systems experienced snow-related power losses over the period that these datasets was collected.

For the utility-scale and string-inverter systems, Mode 0 is achieved when the inverter is unable to reach the turn-on voltage; i.e., too many substrings are covered with effectively opaque snow. We estimate this coverage threshold C_V for each system based on the fraction of the number of substrings operating at $T_{eff} = 1$ necessary to surpass V_{turnon}. Comparisons of modal frequencies and rates of missing timestamps between the two inverter-connected systems and the two single module systems suggest that portrait-orientation systems experience Mode 0 at a higher frequency relative to landscape-orientation modules 4.

Mode 1 describes data with reduced values for both V_{ratio} and T_{eff}. The majority of this data was recorded after snow fell on modules that were already partially covered. We hypothesize that Mode 1 primarily corresponds to full or partial coverage by snow with non-uniform transmission,

TABLE II
SNOW POWER LOSS MODES. EFFECTIVE COVERAGE IS C_{eff}, EFFECTIVE TRANSMISSION IS T_{eff}

	Mode 0	***Mode 1***	***Mode 2***	***Mode 3***	***Mode 4***
C_{eff}	1	1-V_{turnon}/V_{mp0} $\leq$ $C_{eff} < 1$	1-V_{turnon}/V_{mp0} $\leq$ $C_{eff} < 1$	≈ 1	0
T_{eff}	0	< 1	≈ 1	< 1	≈ 1
Physical interpretation	Partial or full coverage by opaque snow, minimum inverter voltage not met	Partial coverage by opaque snow, partial coverage by transmissive snow	Partial coverage by opaque snow, partial uncovered	Partial or full coverage by transmissive snow	Zero coverage or partial or full coverage by highly transmissive snow

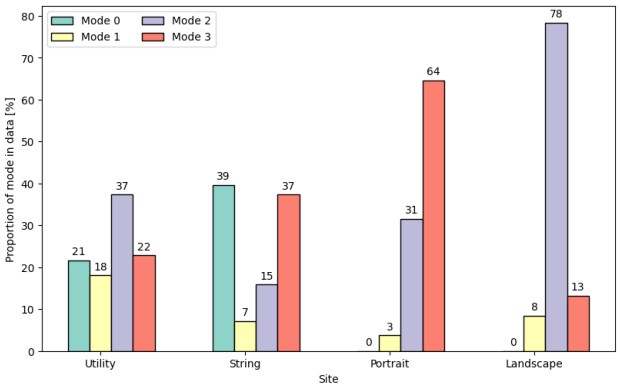

Fig. 5. Relative frequencies of modes for data collected between October and May that includes significant power losses. Data from mode 0 is not collected for the two module-scale systems, but an analysis of missing timestamps found that the portrait-orientation system was offline for $\approx$ 13 hours longer than the landscape-orientation system.

where $1 - V_{ratio}$ is equivalent to the fraction of array surface area covered by opaque snow and T_{eff} is equivalent of the transmission of non-opaque snow partially or fully covering the remaining area. In this line of thinking, Mode 1 is the product of incomplete shedding and the relative frequency of Mode 1 to other modes may be an indicator of performance by site design in facilitating shedding.

Mode 2 is representative of partial coverage by opaque snow with the remaining portion of the array uncovered. If the system is connected to an inverter, partial coverage by opaque snow must be below the coverage threshold for the inverter to turn on. Based on observations of systems experiencing some kind of snow-related power loss, landscape-orientation systems experience Modes 1 and 2 more frequently than portrait-orientation systems 6. Relative to other modes, portrait-orientation modules are more frequently found to be in Mode 3, which describes data where a full or partial cover of transmissive snow decreases effective transmission but all substrings remain active. Mode 4 was observed to correspond to snow-free production or partial or full coverage by a highly transmissive layer of frost or snow, where in either case, little to no power is lost.

Figure 6 compares modal frequencies with attributable power losses at the utility-scale site. Power losses associated with Mode 2 are minimal, which is consistent with high transmission values and low partial coverage. Modes 1 and 3, where $T_{eff} < 1$, lead to significant power losses. Some power losses were observed in Mode 4 - these may be attributable to fog or dew - but they were small relative to the frequency of Mode 4.

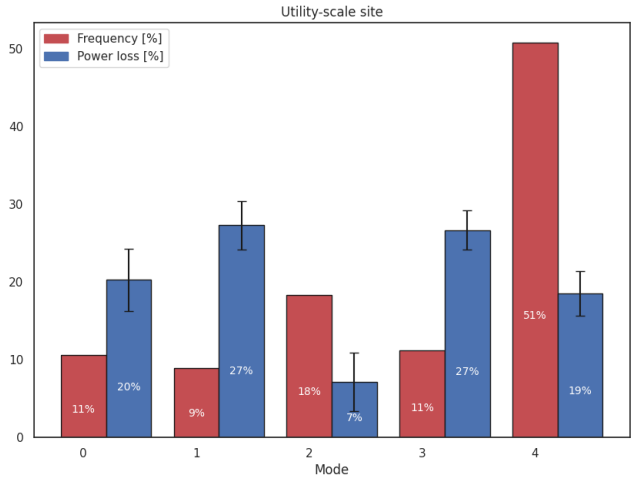

Fig. 6. Frequencies and attributable power losses of modes for all data collected at the utility-scale site between October and May.

CONCLUSION

The introduction and validation of a framework by which snow-related power loss modes can be identified in utility-scale data has the potential to vastly simplify the estimation of power losses and minimize associated requirements for monitoring equipment. Four distinct snow-related power loss modes corresponding to different effective coverage and transmission ranges for snow cover were identified from inverter data at a utility-scale PV site. The presence of snow as detected from electrical data, as well as the physical interpretations of snow cover corresponding to each power loss mode have been verified in time-series images from the site. The modes have been validated using data from inverter-connected and single module research-scale systems, and we observe similar patterns in the relationship between spatial snow cover and snow transmission across systems. We observe significant differences in modal frequencies between landscape and portrait-orientation systems; portrait-orientation systems

tend to be completely offline more frequently, while landscape-orientation systems tend remain online despite partial snow coverage. These differences are consistent with the idea that the majority of partial snow covers obscure a nonzero fraction of each substring on a landscape-orientation module, whereas it is typical for at least one substring to be exposed on a landscape orientation module with partial snow cover. For inverter-connected systems, modes with low or zero transmission values have the largest impact on power, while partial coverage has a minimal impact. Future studies should be performed to explore the impact of other system characteristics on modal frequencies such as tilt angle and location.

REFERENCES

[1] "The challenges of achieving a 100% renewable electricity system in the United States - ScienceDirect." [Online]. Available: https://www.sciencedirect.com/science/article/pii/S2542435121001513

[2] R. E. Pawluk, Y. Chen, and Y. She, "Photovoltaic electricity generation loss due to snow – A literature review on influence factors, estimation, and mitigation," *Renewable and Sustainable Energy Reviews*, vol. 107, pp. 171–182, Jun. 2019. [Online]. Available: https://www.sciencedirect.com/science/article/pii/S1364032118308268

[3] E. Andenæs, B. P. Jelle, K. Ramlo, T. Kolås, J. Selj, and S. E. Foss, "The influence of snow and ice coverage on the energy generation from photovoltaic solar cells," *Solar Energy*, vol. 159, pp. 318–328, Jan. 2018. [Online]. Available: https://www.sciencedirect.com/science/article/pii/S0038092X17309581

[4] R. W. Andrews, A. Pollard, and J. M. Pearce, "The effects of snowfall on solar photovoltaic performance," *Solar Energy*, vol. 92, pp. 84–97, Jun. 2013. [Online]. Available: https://www.sciencedirect.com/science/article/pii/S0038092X13000790

[5] "New England Energy Report." [Online]. Available: https://www.eia.gov/dashboard/newengland/electricity

[6] L. Powers, J. Newmiller, and T. Townsend, "Measuring and modeling the effect of snow on photovoltaic system performance," in *2010 35th IEEE Photovoltaic Specialists Conference*, Jun. 2010, pp. 000 973–000 978, iSSN: 0160-8371.

[7] T. Townsend and L. Powers, "Photovoltaics and snow: An update from two winters of measurements in the SIERRA," in *2011 37th IEEE Photovoltaic Specialists Conference*, Jun. 2011, pp. 003 231–003 236, iSSN: 0160-8371.

[8] J. Braid, D. Riley, and L. Burnham, "Design Considerations for Photovoltaic Systems Deployed in Snowy Climates," *37th European Photovoltaic Solar Energy Conference and Exhibition*, pp. 1626–1631, Oct. 2020, iSBN: 9783936338737 Publisher: WIP. [Online]. Available: http://www.eupvsec-proceedings.com/proceedings?paper=49817

[9] "Most utility-scale fixed-tilt solar photovoltaic systems are tilted 20 degrees-30 degrees." [Online]. Available: https://www.eia.gov/todayinenergy/detail.php?id=37372

[10] M. B. Øgaard, B. L. Aarseth, F. Skomedal, H. N. Riise, S. Sartori, and J. H. Selj, "Identifying snow in photovoltaic monitoring data for improved snow loss modeling and snow detection," *Solar Energy*, vol. 223, pp. 238–247, Jul. 2021. [Online]. Available: https://www.sciencedirect.com/science/article/pii/S0038092X21003868

[11] A. Dolara, G. C. Lazaroiu, S. Leva, and G. Manzolini, "Experimental investigation of partial shading scenarios on PV (photovoltaic) modules," *Energy*, vol. 55, pp. 466–475, Jun. 2013. [Online]. Available: https://www.sciencedirect.com/science/article/pii/S0360544213003095

[12] Z. DeFreitas, G. Binnard, and T. Delsart, "Using On-site Ambient Temperature and Performance Ratio to Identify Days when Snow Cover Affects PV Plant Production," in *2021 IEEE 48th Photovoltaic Specialists Conference (PVSC)*, Jun. 2021, pp. 1860–1864, iSSN: 0160-8371.

[13] A. Livera, M. Theristis, E. Koumpli, S. Theocharides, G. Makrides, J. Sutterlueti, J. S. Stein, and G. E. Georghiou, "Data processing and quality verification for improved photovoltaic performance and reliability analytics," *Progress in Photovoltaics: Research and Applications*, vol. 29, no. 2, pp. 143–158, 2021, _eprint: https://onlinelibrary.wiley.com/doi/pdf/10.1002/pip.3349. [Online]. Available: https://onlinelibrary.wiley.com/doi/abs/10.1002/pip.3349

[14] J. L. Braid, D. Riley, J. M. Pearce, and L. Burnham, "Image Analysis Method for Quantifying Snow Losses on PV Systems," in *2020 47th IEEE Photovoltaic Specialists Conference (PVSC)*, Jun. 2020, pp. 1510–1516, iSSN: 0160-8371.

[15] D. L. King, W. E. Boyson, and J. A. Kratochvill, "Photovoltaic Array Performance Model."